Eur Biophys J (2006) 35: 181–189
DOI 10.1007/s00249-005-0015-9

ARTICLE

Herbert Schmiedel · László Almásy · Gotthard Klose

Multilamellarity, structure and hydration of extruded POPC vesicles by SANS

Received: 7 June 2005 / Revised: 2 August 2005 / Accepted: 25 August 2005 / Published online: 8 November 2005

Abstract The small-angle neutron scattering (SANS) data of 12 1-palmitoyl-2-oleoyl-*sn*-glycero-3-phosphocholine (POPC) dispersions at low lipid concentration (1 mg per 100-mg heavy water) prepared by 5, 9 and 29 extrusions through filters of pores with 50, 100, 200 and 400 nm diameter are presented. They were analyzed within a theory that permits the determination of both structural and hydration parameters of the bilayers as well as the portions of multilamellar vesicles in dispersions with negligible long-range order between the vesicles. The scattering length density profile across the bilayers is approximated by assuming a central hydrocarbon core surrounded by a water-accessible coat. It is modeled by two different forms of functions. In the boat model, the scattering length density of the coat changes linearly from core to water, whereas in the strip model it is constant across the water-accessible coat. It was found that the boat model reflects the reality better than the strip model. The decrease of the multilamellar vesicle portions, either with increasing the number of extrusions at same filter size and with decreasing the filter size, was characterized quantitatively.

Keywords SANS · POPC · Vesicles · Extrusion · Multilamellarity

Introduction

Unilamellar lipid vesicles consist of closed single lipid bilayers separating outer and inner compartments. The single molecular bilayer in such vesicles is a more realistic model of a biological membrane than multilamellar systems (Schmiedel et al. 2001; Hope et al.1985). There is a large variety of procedures for preparing vesicle dispersion such as extrusion and others (New 1990; Hallett et al. 1991; Engelhaaf et al. 1996, and references therein). They yield dispersions of vesicles with a size distribution (polydispersity) and with different numbers of bilayers. We denote the existence of multilamellar vesicles besides unilamellar vesicles in the following as multilamellarity. Both polydispersity and multilamellarity depend on the external conditions as well as on lipid composition and solvent. For instance, using extrusion procedure, Cornell et al. (1981) found that the average diameter of the vesicles changes relatively little with temperature, even across the main phase transition temperature. Repeated extrusion under relatively high pressure reduces the vesicle size distribution and increases the trapping efficiency (Hope et al.1985; Mayer et al.1986). Mayer et al. (1986) reasoned and demonstrated qualitatively that filtering with larger pore size results in vesicle dispersions with increased multilamellar character. The addition of surface active compounds increases the tendency for formation of unilamellar vesicles (Gabriel and Roberts 1984; Fromherz 1983). Dispersions of pure 1-palmitoyl-2-oleoyl-*sn*-glycero-3-phosphocholine (POPC) prepared by repeated (30 times) extrusion through polycarbonate membranes with 200-nm pores at room temperature contain multilamellar vesicles, the amount of which reduces drastically with increasing amount of tetra (ethylene oxide) mono dodecyl ether ($C_{12}E_4$) over 0.5 surfactant molar fraction (Schmiedel et al. 2001). The tendency for forming unilamellar lipid vesicles also increases if one uses sucrose solution instead of pure water as solvent (Kiselev et al. 2001).

There are many papers available reporting about the elucidation of vesicle size distribution using various methods such as electron microscopy, light scattering, ultracentrifugation, gel filtration, and small angle neutron scattering [for references see, e.g., Hallett et al. (1991); Engelhaaf et al. (1996), and references therein].

H. Schmiedel · G. Klose (✉)
Faculty of Physics and Earth Science Institute for Experimental Physics I, University Leipzig, Linnéstr. 5, 04103 Leipzig, Germany
E-mail: klose@physik.uni-leipzig.de

L. Almásy
Research Institute for Solid State Physics and Optics, POB 49, Budapest, 1525 Hungary

But to date, there is no paper published devoting to the multilamellarity, according to our knowledge.

The objective of the present study is the quantitative determination of the multilamellar portions in extruded POPC vesicle dispersions, extending the method proposed in our recent paper (Schmiedel 2001), in which we assumed that in extruded POPC dispersions only unilamellar and bilamellar vesicles are present. Now we take into account multilamellar vesicles not only of two (as in Schmiedel et al. 2001), but also of three and more bilayers, and study the behavior of the resulting parameters in function of the number of extrusions and the pore size. The quality of the fitted curves to the scattering data is much better. Further, we will show that the multilamellarity determined from small-angle neutron scattering (SANS) is relatively insensitive to the scattering length density profile assumed across the bilayer. The analysis of the scattering yields quantitatively the same multilamellarity for the strip model used in Ref. (Schmiedel 2001) and for a profile where the scattering length density across the coat region of the membrane changes linearly (see below). We denote the latter as boat model; remarkably, it yields the same level of fitting accuracy as the strip model though it contains one fitting parameter less than the strip model (see below). Finally, we will show that the analysis also yields reasonable results of the multilamellarity in case of only a few percent of multilamellar vesicles in the dispersions.

Material and methods

Substances and preparation of the vesicle dispersions

The lipid POPC was purchased as powder from Avanti Polar Lipids/USA and used without further purification. Deuterium oxide (D_2O) was obtained from Chemotrade/Germany.

The lipid was put in an ampoule with 99.9% heavy water (10 mg/1 ml) which was vortexed for some minutes, resulting in a macroscopically homogeneously looking dispersion of crude multilamellar vesicles. Lots of this stock dispersion were carefully filled into a hand extruder (LiposoFast Basic AVESTIN Inc. Canada) for avoiding air cavities and then extruded through two polycarbonate filters (Milsch Equipment, Germany) at room temperature. After that the dispersions of prevailing unilamellar vesicles obtained were stored for 1 h under a pressure of 6.5 kPa. The samples prepared in this way are stable across at least 10 h according to measurements of light transmission. They were prepared immediately before starting the SANS experiments.

Altogether 12 samples were prepared by applying 5, 9 and 29 extrusions and by using polycarbonate filters with pores of 50, 100, 200 and 400 nm diameters.

The mean distance between nearest neighboring vesicles in the prepared dispersions is similar to the vesicle radius or bigger. There is no long-range order between the bilayers of different vesicles.

SANS measurements

The SANS measurements were performed with the small-angle neutron scattering diffractometer "Yellow Submarine" operating on the cold neutron beam line at the Budapest Research Reactor (Rosta 2002). A mean neutron wavelength $\lambda = 0.4$ nm, and sample-detector distances 1.5 and 4.5 m were used, covering the scattering vector range 0.21–3.6 nm^{-1}. The acquisition times were between 60 and 150 min for each sample at each detector position. The samples were filled in quartz cells (Hellma/Germany) with a sample thickness of 1 or 2 mm, and thermostated at 25 ± 0.1°C.

The scattered neutrons were registered by a two-dimensional position sensitive detector with pixel size 1×1 cm^2. The raw data were azimuthally averaged and grouped to about 30 points equidistant in scattering length q. The obtained raw scattering data were corrected for the detector sensitivity, the room background, the scattering of an empty cell, and the transmission of the sample by standard procedures.

Data analysis

Models

Strip model

The neutron scattering length density profile of a vesicle consisting of three bilayers ($M = 3$) is presented in Fig. 1a for the strip model. The fundamental motif of this density profile is the water-free core of thickness c in the center of each bilayer, surrounded by the water-accessible coat of thickness h followed by the interbilayer water layer of thickness d_w. In a vesicle consisting of M bilayers, this motif is repeated M times. It is assumed that the neutron scattering length density of the central core is fixed to be $\rho_c = -0.36\times10^{14} m^{-2}$ which corresponds to a typical hydrocarbon. The scattering length density of the interbilayer water layer is that of pure heavy water, $\rho_s = 6.36\times10^{14}\ m^{-2}$. The neutron scattering length density ρ_h of the water-accessible coat, together with the lengths c, h, d_w, are fitting parameters. It should be emphasized once more that the coat comprises the region of the bilayer that differs in scattering length density both from pure hydrocarbon and pure D_2O. Therefore, besides the head-groups, the coat comprises also a part of the acyl chains of the lipid molecules since water is penetrating towards the core; in other words, the coat is not identical to the hydrophilic head group region, as discussed in many papers concerning artificial membranes.

Boat model

In the boat model, a linear change of the scattering length density across the coat region is assumed

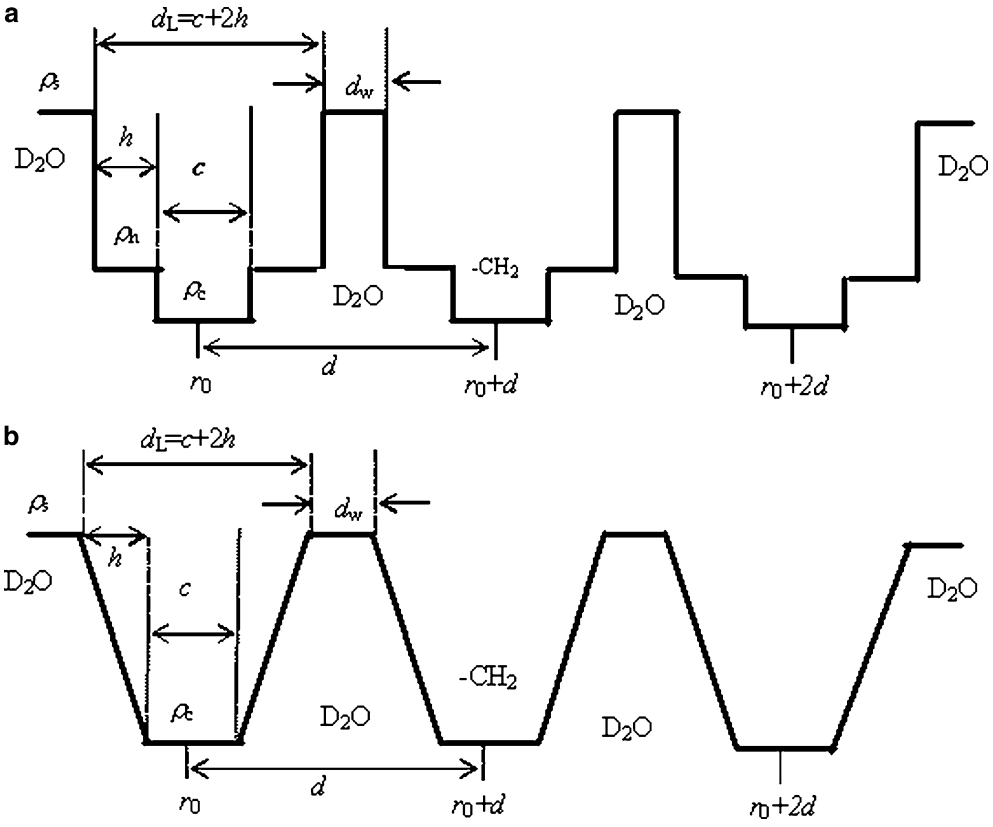

Fig. 1 Schematic drawing of the scattering length density profile across the membranes of a multilamellar vesicle with three bilayers used to simulate SANS intensities of vesicle dispersions for the strip model (**a**) and for the boat model (**b**)

(cf. Fig. 1b). The model has one fitting parameter less than the strip model; namely, only three adjustable parameters, the thicknesses of the hydrophobic core c, of the water accessible coat h, and of the water layer d_w.

Theoretical scattering function

The average coherent neutron differential cross-section of the M-bilayer vesicles in the case of large vesicle radii and negligible long-range order between the vesicles is according to Appendix 1 given by the formula:

$$\left(\frac{d\sigma}{d\Omega}\right)_M = \left(\frac{4\pi}{q}\right)^2 \langle r_{0M}^2 \cdot \sin^2(q \cdot r_{0M})\rangle \rho(q)^2 \cdot \left[\frac{\sin\left(q \cdot M \cdot \frac{d}{2}\right)}{\sin\left(q \cdot \frac{d}{2}\right)}\right]^2 \equiv I_M^{\mathrm{coh}}(q, R, c, h, d_w, \rho_h) \quad (1)$$

(the parameter ρ_h is absent in the boat model) where

$$\rho(q) = \frac{2}{q} \cdot \left[(\rho_h - \rho_s)\sin\left(q \cdot \frac{d_L}{2}\right) + (\rho_c - \rho_h) \cdot \sin\left(q \cdot \frac{c}{2}\right)\right] \equiv \rho^{\mathrm{strip}}(q) \quad (2a)$$

and

$$\rho(q) = \frac{2}{q} \cdot (\rho_c - \rho_s)\left[\sin\left(q \cdot \frac{c}{2}\right) \cdot \frac{\sin(q \cdot h)}{q \cdot h} + \cos\left(q \cdot \frac{c}{2}\right)\right] \cdot \frac{\left(1 - \cos\left(q \cdot \frac{h}{2}\right)\right)}{q \cdot h} \equiv \rho^{\mathrm{boat}}(q) \quad (2b)$$

are the form factors of a single bilayer in case of strip and boat models, respectively. q is the length of the scattering vector, $d_L = c + 2 \cdot h$ is the bilayer thickness and $d = d_L + d_w$ is the repeat distance. The brackets in (1) denote the averaging over the distribution of vesicle radii $r_{0M} = r_0 + (M - 1) \cdot d/2$, where r_0 is the midpoint radius of the innermost bilayer in the vesicle (see Fig. 1). In deriving (1) it was assumed that $r_{0M} >> d$ ("large" vesicle radius). The interference factor

$$\left[\frac{\sin\left(q \cdot M \cdot \frac{d}{2}\right)}{\sin\left(q \cdot \frac{d}{2}\right)}\right]^2$$

in (1) gives the well-known main diffraction peaks characteristic of multilamellar samples by increasing the number M of bilayers in the vesicles .

As had been proved by electron microscopy (Schmiedel et al. 2001; Hallet et al. 1991), the radius distribution of extruded vesicles can be approximated by the nonsymmetrical Schulz distribution

$$G(r) = \left(\frac{m+1}{R}\right)^{m+1} \cdot \frac{r^m}{m!} \cdot \exp\left[\frac{(m+1)\cdot r}{R}\right] \tag{3}$$

with $m = 3$ and $2R$ is the pore diameter of the filters applied for extrusion. The shape of the scattering curves in the studied q-range is rather insensitive to the actual polydispersity and to the form of the size distribution function. Therefore, we use (3) with fixed parameters, evaluating the average in (1) analytically, as it is shown in Appendix 2.

The experimentally obtained neutron scattering intensity $I^{\exp}{}_{\mathrm{V}}(q_0)$ at scattering vector q_0 of extruded vesicle dispersions is approximated by the following formula:

$$\begin{aligned} I_V^{\mathrm{theo}}(q_0) &= I_{\mathrm{Bg}}^{\mathrm{inc}} + \sum_{M=1}^{M_{\max}} g_M \\ &\quad \cdot \int_{q_0-3\sigma_q(q_0)}^{q_0+3\sigma_q(q_0)} \mathrm{d}q \cdot f(q_0,q).I_M^{\mathrm{coh}}(q_0-q,R,c,h,d_w,\rho_h) \\ &\approx I_V^{\exp}(q_0) \end{aligned} \tag{4}$$

$I^{\mathrm{inc}}{}_{\mathrm{Bg}}$ is the q-independent background caused mainly by incoherent scattering originating from the hydrogen nuclei in the vesicles and the heavy water. In the fitting procedure, this background term was fixed to the asymptotic value of $I^{\exp}{}_{\mathrm{V}}(q_0)$ (average value of $I^{\exp}{}_{\mathrm{V}}(q_0)$ for large values of q_0, in our case $q_0 > 3\ \mathrm{nm}^{-1}$).

In (4), the coherent scattering intensity of the vesicles is convoluted with the resolution function $f(q_0, q)$ of the instrument. It was calculated following the approach of Pedersen et al. (Pedersen et al 1990), where the contributions of finite angular resolution and the wavelength distribution are taken into account. $\sigma_q(q_0)$is the width of the resolution function at each given q_0.

The parameters g_M ($M = 1, 2, ..., M_{\max}$) are the portions of the M-bilayer vesicles present in the dispersion. These parameters, together with c, h, d_{w} and ρ_h form a set of $M_{\max} + 4$ (strip model) or $M_{\max} + 3$ (boat model) fitting (adjustable) parameters.

Fitting procedure

The scattering intensity varies over almost three orders of magnitude in the experimental q-range. The information about the structural and hydration parameters and the multilamellarity are mainly determined by the central part of the scattering curve, where the diffraction-like bump appears . Since the experimental error bars in this part are much bigger than that at low q, the usual least squares fitting to the intensities underestimates the contribution of the central part of the spectrum. Therefore, for obtaining our parameters, the following objective function was minimized:

$$\sum_k \left[\lg\left(I_V^{\exp}(q_k)\right) - \lg\left(I_V^{\mathrm{theo}}(q_k)\right)\right]^2 \cdot \frac{I_V^{\exp}(q_k)}{\Delta I_V^{\exp}(q_k)} \rightarrow \text{minimum}.$$

$\Delta I^{\exp}{}_{\mathrm{V}}(q_k)$ is the standard deviation of the measured scattering intensity $I^{\exp}{}_{\mathrm{V}}(q_k)$at point q_k. The minimization procedure used in our fit program is the simplex method described by Nelder and Mead (1965).

The errors of the obtained parameters have been estimated in the following way. The fitting procedure was carried out under the additional condition that the theoretical curve and the experimental data exactly agree at two q values. The theoretical curve $I^{\mathrm{theo}}{}_{\mathrm{V}}(q_0)$ was forced to exactly fit the asymptotic value, $I^{\mathrm{inc}}{}_{\mathrm{Bg}}$, and the experimental intensity, $I^{\exp}{}_{\mathrm{V}}(q_k)$, at another q_0 value in the low q region, where a steep descend of the scattering intensity is observed. The fit results scatter depending on the point q_k that is chosen to be exactly fitted. For instance, in case of the dispersion prepared by 29 extrusions through filters with 50-nm pores, the values of the parameter c for the thickness of the water-free membrane core lies in the range from 2.1 to 1.91 nm choosing the first 13 experimental data from 0.0175 to 0.0558 A^{-1} (cf. Fig. 2) at q_k. In this manner, we have chosen the first 13 experimental data points at lowest q_k ($k = 1, 2, ..,13$). From the results of these fits, the mean values of the fit parameters and their standard deviations have been determined.

The quality of a single fit can be defined as the normalized sum of the absolute values of the deviations of the experimental data from the fit, i.e.,

$$\mathrm{CHI}\% = \frac{\sum_k \left|\lg\left(I_V^{\exp}(q_k)\right) - \lg\left(I_V^{\mathrm{theo}}(q_k)\right)\right|}{\sum_k \left|\lg\left(I_V^{\exp}(q_k)\right)\right|} \cdot 100\%. \tag{5}$$

In analogy to the mean structural and hydration parameters, the *mean* quality of all our fits of a given scattering curve is the average of the 13 CHI% values obtained in the single fits.

Hydration parameters

The number of water molecules per lipid molecule in the coat region in case of strip/boat models, $N^{\mathrm{strip/boat}}{}_{\mathrm{w}}$, and the area requirements, $A^{\mathrm{strip/boat}}$, per lipid molecule are obtained from the quantities c, h and ρ_h using the following formulas:

$$\begin{aligned} N_{\mathrm{w}}^{\mathrm{strip}} &= \frac{V_{\mathrm{L}} \cdot (2h\rho_h + c\rho_{\mathrm{c}}) - d_{\mathrm{L}} b_{\mathrm{L}}}{b_{\mathrm{w}} d_{\mathrm{L}} - V_{\mathrm{w}} \cdot (2h\rho_h + c\rho_{\mathrm{c}})}, \\ N_{\mathrm{w}}^{\mathrm{boat}} &= \frac{V_{\mathrm{L}} \cdot [c\rho_c + h(\rho_{\mathrm{s}} - \rho_{\mathrm{c}})] - d_{\mathrm{L}} b_{\mathrm{L}}}{b_{\mathrm{w}} d_{\mathrm{L}} - V_{\mathrm{w}} \cdot [c\rho_c + h(\rho_{\mathrm{s}} - \rho_c)]} \end{aligned} \tag{6a}$$

and

$$A^{\mathrm{strip/boat}} = \frac{2 \cdot \left(N_{\mathrm{w}}^{\mathrm{strip/boat}} V_{\mathrm{w}} + V_{\mathrm{L}}\right)}{d_{\mathrm{L}}}. \tag{6b}$$

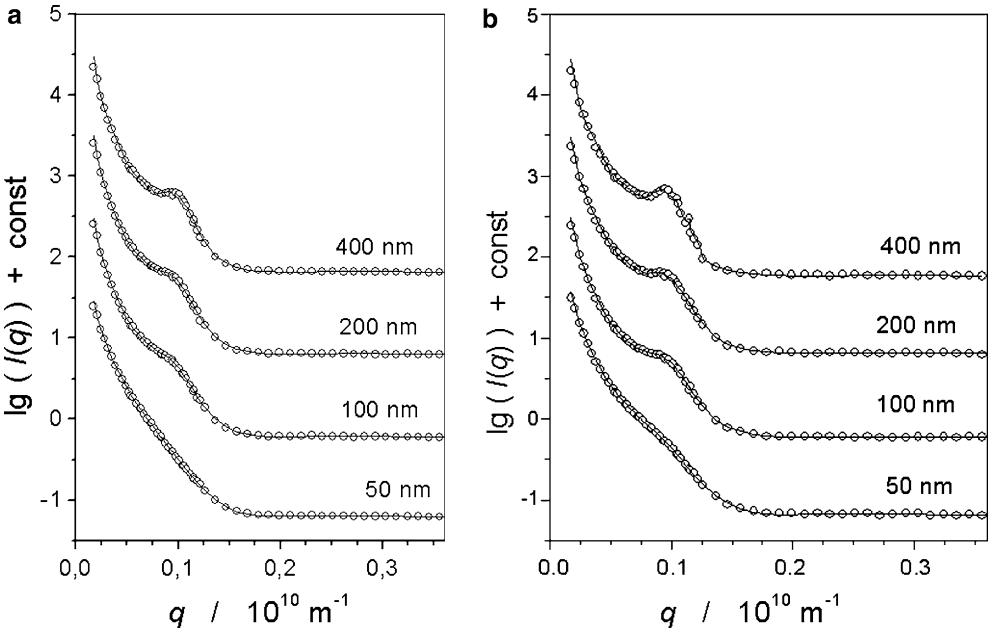

Fig. 2 **a** Experimental SANS data (*open circles*) obtained from POPC dispersions prepared by 29 extrusions through two polycarbonate filters with 50, 100, 200 and 400 nm pores and theoretical curves obtained by our approach (see text) using the boat model and including vesicles up to maximum four bilayers in the fitting procedure. **b** Experimental SANS data obtained from POPC dispersions prepared by five extrusions through two polycarbonate filters with 50, 100, 200 and 400 nm pores and theoretical curves obtained by our approach (see text) using the boat model and including vesicles up to maximum four bilayers in the fitting procedure

V_w and V_L are the molecular volumes of water and lipid (POPC), respectively, and b_w and b_L are the total coherent scattering lengths of a water and of a lipid molecule, respectively. Equations (6) are obtained from the balance equations for the total volume and the total scattering length of the "elementary cell" of the bilayer, consisting of two lipid molecules and $2{\cdot}N_w$ water molecules in the volume $A{\cdot}d_L = A{\cdot}(c + 2{\cdot}h)$.

Results and discussion

In Fig. 2a, b the experimental scattering data are presented together with the theoretical curves obtained by the above-described fitting procedure for the boat and the strip models assuming up to tetralamellar (M_{max} = 4) vesicles in the POPC dispersions. The fitting curves for the strip and the boat models cannot be distinguished by eye.

The shoulder or hump of the scattering curves near $q \approx 1$ nm^{-1} (cf. Fig. 2a, b) is due to interference effects resulting from multilamellar vesicles or/and (unilamellar) vesicle aggregates. The position of the scattering hump (cf. d in Table 1) is almost independent of vesicle size and the number of extrusions. Further, its size and width correlate well with the pore diameter of the extrusion filter and the number of extrusions. Therefore, we interpret the growing appearance of the hump with growing vesicle size as being caused by an increasing percentage of multilamellar vesicles in the samples. In our model, these quantities are described by the parameters g_1, g_2, g_3 and g_4. It is remarkable that both strip and boat models deliver the same multilamellarity parameter $p_m \equiv 1 - g_1 \approx \sum_{i=2}^{4} g_i$ within approximately one

Table 1 Parameters (mean values) obtained within our approach (see text) using the boat model and including vesicles up to maximum four bilayers for POPC dispersions prepared by 5, 9 and 29 extrusions through two polycarbonate filters with 50, 100, 200 and 400 nm pores

$2R$/nm	N_{ext}	g_1	g_2	g_3	g_4	CHI%	c/nm	h/nm	d_L/nm	d_w/nm	d/nm	N_w	A/nm^2
400	5	0.710	0.111	0.014	0.165	2.95	1.85	1.17	4.20	2.07	6.26	13.1	0.79
	9	0.706	0.099	0.015	0.180	3.10	1.88	1.15	4.18	2.07	6.25	12.7	0.79
	29	0.779	0.095	0.012	0.114	2.21	2.13	1.04	4.21	2.03	6.24	10.4	0.75
200	5	0.770	0.124	0.015	0.091	1.76	2.06	1.08	4.23	2.07	6.30	11.2	0.76
	9	0.783	0.134	0.014	0.089	1.68	2.17	1.02	4.22	2.10	6.32	10.1	0.74
	29	0.806	0.123	0.015	0.057	1.56	2.01	1.18	4.38	1.97	6.35	12.3	0.75
100	5	0.802	0.123	0.020	0.055	1.54	1.95	1.20	4.34	2.01	6.35	12.9	0.76
	9	0.812	0.130	0.016	0.041	1.40	2.16	1.07	4.30	2.07	6.37	10.6	0.74
	29	0.838	0.121	0.011	0.030	1.21	2.08	1.16	4.40	1.97	6.37	11.7	0.73
50	5	0.923	0.064	0.004	0.008	1.17	2.28	1.08	4.43	2.07	6.50	10.1	0.71
	9	0.945	0.046	0.002	0.008	1.18	2.23	1.14	4.50	1.96	6.46	10.9	0.71
	29	0.983	0.015	0.002	0.001	1.08	2.04	1.34	4.71	1.89	6.60	13.5	0.71

g_i are the number fractions of vesicles with i bilayers; CHI% is the quality parameter of the fit (see text); c, h, d_L, are the thickness of the water-free core, of the water-accessible coat, and of the lipid bilayers, respectively. A is the lipid area and N_w is the number of water molecules per lipid molecule incorporated in the bilayer. Finally, d_w is the thickness of the water layer between adjacent membranes and d the repeat distance in multilamellar vesicles

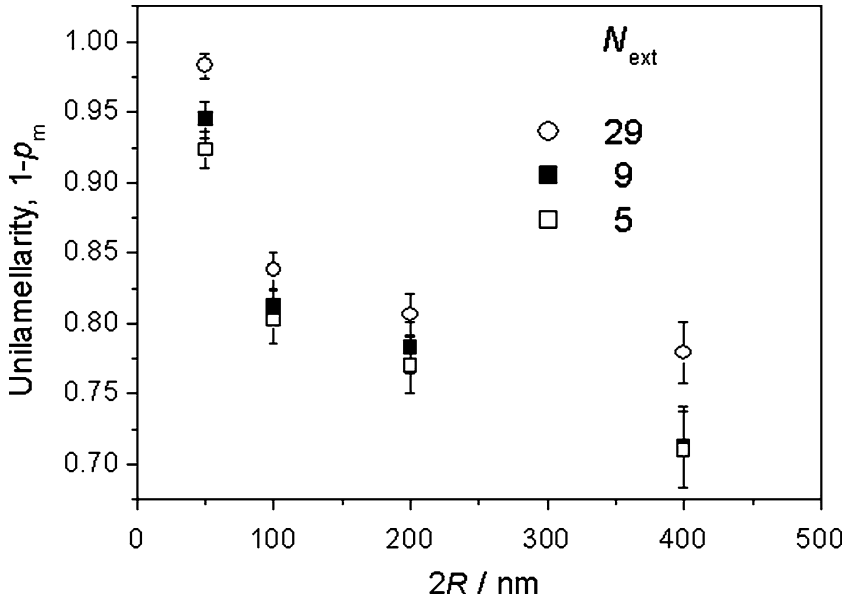

Fig. 3 Unilamellarity, $1 - p_m$, (see text) of POPC dispersions versus filter pore size. The increase in the multilamellarity parameter, p_m, with increasing pore radius diameter $2R$ and number of extrusions, N_{ext}, is clearly visible

percent accuracy for all samples prepared with the same number N_{ext} of extrusions and with the same pore diameter $2R$ of the extrusion filter.

Table 1 lists fitting results obtained from the 12 samples prepared by $N_{ext} = 5$, 9, and 29 extrusions through two polycarbonate filters of $2R = 50$, 100, 200, and 400 nm pore diameters. Because of the uncertainties

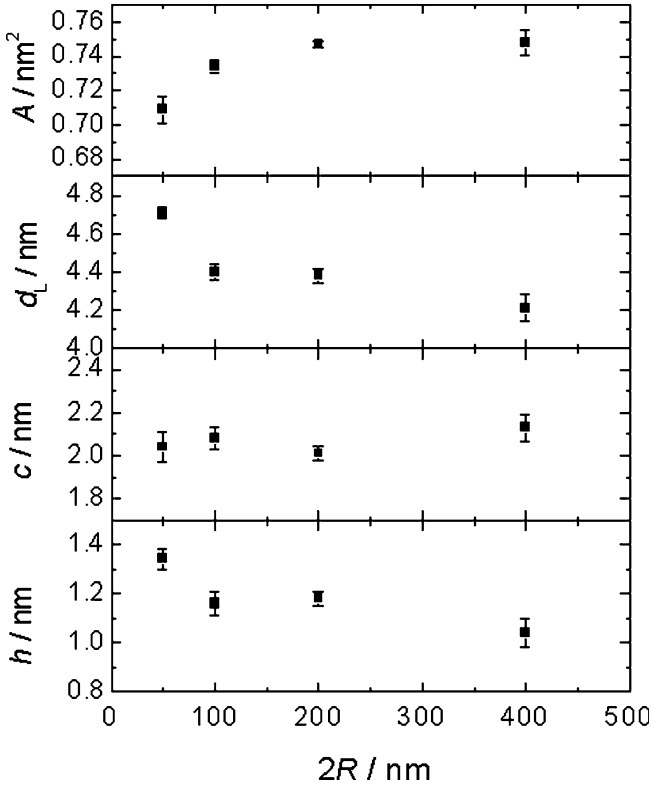

Fig. 4 Thicknesses of the membrane coat h, of the membrane core c, and of the bilayer d_L, and the lipid area A for vesicle dispersions prepared by 29 extrusions through two filters as function of the pore diameter $2R$ of extrusion filter

(cf. Figs. 3, 4, 5), only two digits of the values for the structural, hydration, and g values are of significance. Only results obtained with the boat model are listed since the boat model exhibits a better convergence of the fitting procedure and it reflects better the true scattering length density profile than the strip model. The latter statement is supported by the following finding. If one superimposes the 13 theoretical scattering length density profiles of the strip model obtained by the procedure for the error estimation described in the preceding paragraph, then the averaged curve becomes rather similar to that of the boat model. On the other hand, the same averaging procedure applied to the boat model results again in a boat form of the scattering length density profile. Therefore, the real scattering length density profile across the bilayer seems to resemble much more that of the boat model than that of the strip model (cf. Fig.1).

The results collected in Table 1 were obtained by taking into account only up to tetralamellar vesicles into the fitting [$M_{max} = 4$, cf. Formula (4)]. To show the effect of the inclusion of different numbers of bilayers into the model vesicles, the fitting was performed also by considering $M_{max} = 5$ and 6. For example, the fitting results for the sample prepared by five extrusions through 400-nm filters (highest multilamellarity) are collected in Table 2. As can be seen, the mean value of CHI% in that case decreases monotonically if one includes multilamellar vesicles with more and more bilayers up to $M_{max} = 6$. The improvement of the fit by increasing M_{max} is thus far not so evident for samples with lower multilamellarity, e.g., for samples prepared by extrusions through 50-nm filters where the value of CHI% remains nearly constant starting with $M_{max} = 2$. In other words, the inclusion of tri-, tetra- and higher lamellar vesicles in this case does not improve the fit. This means that in case of the sample with 400-nm vesicles, we should have considered vesicles with more

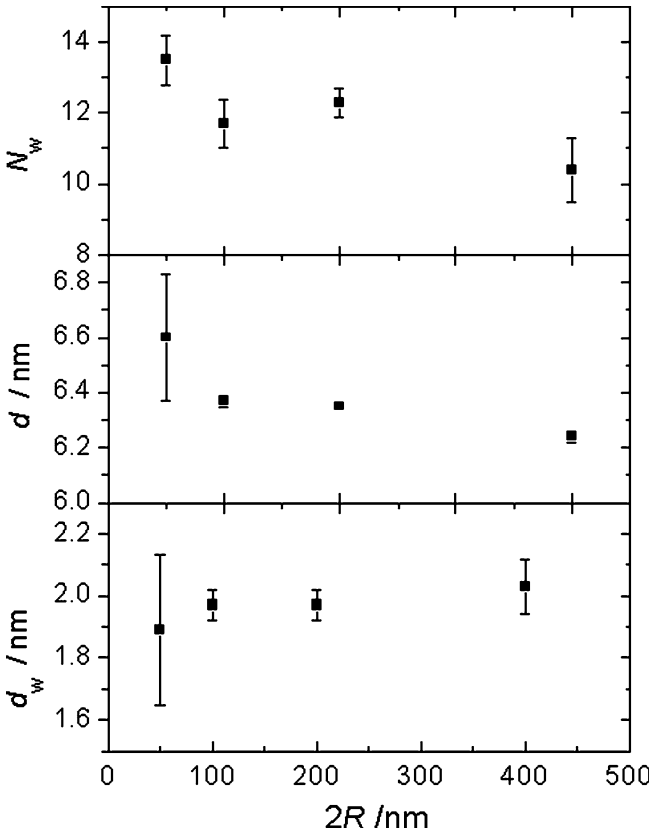

Fig. 5 Thickness of the water layer between adjacent bilayers in multilamellar vesicles d_w, repeat distance d, and amount of water included into the membrane coat N_w for vesicle dispersions prepared by 29 extrusions through two filters via pore diameter $2R$ of extrusion filter

than six bilayers. But the introduction of still more fitting parameters in our approach has no sense at the given quality of our experimental data. On the other hand, if one takes into account only bilamellar vesicles, the fitting yields senseless structural and hydration parameters (cf. first row in Table 2). Therefore, a reasonable compromise for our samples prepared by 5, 9 and 29 extrusions through filters with 50, 100, 200 and 400 nm pores is by the use of $M_{max} = 4$ in all fits as was done in Table 1.

Further, as can be seen from Table 2, the structural and hydration parameters change only little, increasing M_{max} from 4 to 6 (cf. Table 2). The changes are negligible in case of samples prepared by 29 extrusions. In Fig. 3 the complement of the multilamellarity parameter, 1-p_m, i.e., the unilamellarity, is represented in dependence of the vesicle size. The multilamellarity, p_m, increases with increasing pore diameter $2R$ of the filters and with decreasing number of extrusions, N_{ext}, applied in vesicle preparations. For instance, in samples prepared with 29 extrusions, p_m increases from 2% up to 22% if one increases the pore diameter $2R$ of the extrusion filters from 50 to 400. In 400-nm vesicle dispersions, the multilamellarity decreases from 29 to 22% if one increases the number of extrusions from 5 to 29. These changes are significant, and the trends are similar for all the investigated pore sizes and numbers of extrusions.

Now we will consider the parameters reflecting structural and hydration properties. Figures 4 and 5 show structural and hydration parameters from samples prepared with 29 extrusions as function of the vesicle size. The thickness of the membrane coat h and the membrane thickness d_L decrease with increasing vesicle size $2R$, whereas the lipid area A increases (cf. Fig. 4). The increase of d_L is mainly due to the change of the thickness of the coat h since the thickness of the membrane core c remains almost constant. The increase of the lipid area A is compatible with the decrease of the membrane thickness d_L. Though these changes are relatively small, they are bigger than the estimated error bars. Figure 5 shows the behavior of the other calculated parameters. The repeat distance d exhibits a decrease with increasing vesicle size which is due to the reduction of the bilayer thickness d_L (cf. Fig. 4) since the water layer thickness d_w remains constant in the limit of errors. The large parameter uncertainties obtained for the 50-nm vesicles is reasonable because the dispersion contains only 2% multilamellar vesicles in contrast to the 400-nm vesicle dispersion with 22% multilamellar vesicles (see above). The amount of water which is incorporated into the coat, N_w, exhibits a tendency to decrease with increasing vesicle size according to Fig. 5. We do not know to which degree these behaviors of the structural and hydration parameters as function on vesicle size reflect the reality since there are no additional experimental data available in literature up till now according to our knowledge.

A discussion of the structural and hydration parameters as function of number of extrusions has no sense since the parameter uncertainties are partially much bigger for samples prepared by five and nine extrusions compared with those prepared by 29 extrusions.

Table 2 Parameters (mean values) obtained within our approach using the boat model for vesicles of different maximum numbers of bilayers (M_{max}) which have been taken into account in the fitting for POPC dispersions prepared by $N_{ext} = 5$ extrusions through two polycarbonate filters with $2R = 400$ nm pores: $M_{max} = 2$ (first row) up to $M_{max} = 6$ (last row)

G_1	g_2	g_3	g_4	g_5	g_6	CHI%	c/nm	h/nm	d_w/nm	d_L/nm	d/nm	N_w	A/nm^2
0.682	0.318					7.83	2.66	0.04	3.47	2.74	6.21	−3.3	0.851
0.688	0.107	0.205				4.86	2.16	0.78	2.51	3.73	6.24	7.6	0.8
0.71	0.111	0.014	0.165			2.95	1.85	1.17	2.07	4.2	6.26	13.1	0.79
0.729	0.12	0.013	0.011	0.127		2.17	1.99	1.12	2.06	4.22	6.28	11.9	0.768
0.744	0.133	0.012	0.006	0.013	0.091	1.89	2.03	1.07	2.12	4.16	6.29	11.2	0.769

Conclusions

The fit of the SANS curves using boat and strip models yields about the same accuracy. However, the boat model compared with the strip model reflects better the real neutron length density profile across the lipid bilayer in unilamellar and multilamellar vesicles and exhibits better convergence behavior in the fit of SANS data. Therefore, the boat model is preferred. The multilamellarity determined by our approach is almost independent on the model used for the neutron length density profile across the bilayer. Therefore, we conclude that the obtained changes of the multilamellarity parameter, p_m, reflect the reality. Inclusion of more and more bilayers into the model improves the fitting quality, especially for big vesicle sizes, but it makes sense only if the quality of the experimental data is considerably improved simultaneously (e.g. statistics, aggregation and sedimentation behavior of the samples). The multilamellarity in POPC dispersions decreases with decreasing pore size of the filters and with increasing number of extrusions. In POPC vesicle dispersions prepared by 29 extrusions through two filters with 50- and 400-nm pores, the quantitative values of the multilamellarity, p_m, are 2 and 22%, respectively. The thickness of the membrane coat h, the bilayer thickness d_L, the repeat distance d, and the amount of water which is incorporated into the coat N_w decrease and in contrast to these the lipid area A increases with increasing vesicle size, whereas the other two parameters (c, d_w) are independent or almost independent of the vesicle size in the limit of errors. This behavior of the parameters has to be considered if one compares the results obtained from dispersions of 50-nm vesicles with those of bigger vesicles.

In the frame of our approach, we obtained the following structural and hydration parameters for the sample prepared by 29 extrusions through two 50-nm filters : thickness of the membrane core $c = 2.04$ nm, thickness of the membrane coat $h = 1.34$ nm, membrane thickness $d_L = 4.71$ nm, lipid area $A = 0.71$ nm^2, water layer thickness between adjacent membranes in multilamellar vesicles $d_w = 1.89$ nm, repeat distance $d = 6.60$ nm.

Acknowledgements This work has been supported by Bundesministerium für Bildung und Forschung (BMBF grant DUBLEI 03) and the EU, contract HPRI-CT-1999-00099 Budapest.

Appendix 1: Derivation of Eq (1)

The neutron coherent scattering amplitude of the M-vesicle depicted in Fig. 1 is given by

$$F_M(q) = \sum_{m=0}^{M-1} F_m(q), \tag{7}$$

where

$$F_m(q) = \frac{4\pi}{q} \cdot \int_{(d_L/2)}^{d_L/2} (r_m + x) \cdot \sin[q \cdot (r_m + x)] \cdot \rho(x)\mathrm{d}x = \frac{4\pi}{q} \cdot \left(\frac{-\partial}{\partial q}\right) \int_{(d_L/2)}^{d_L/2} \cos[q \cdot (r_m + x)] \cdot \rho(x)\mathrm{d}x \tag{8}$$

is the form factor of the m-th bilayer in the vesicle. $r_m = r_0 + m \cdot d$ is the midpoint radius of that bilayer, and the scattering length density difference between the membrane and the solvent is described by $\rho(x)$ at point x. As the bilayers in Fig. 1 are assumed to be symmetric, i.e.,

$$\rho(-x) = \rho(x), \tag{9}$$

we obtain for the integral in (8)

$$F_m(q) = \tfrac{4\pi}{q} \cdot \int_{(d_L/2)}^{d_L/2} (r_m + x) \cdot \sin[q \cdot (r_m + x)] \cdot \rho(x)\mathrm{d}x = \tfrac{4\pi}{q} \cdot \left(\tfrac{-\partial}{\partial q}\right) \int_{(d_L/2)}^{d_L/2} \cos[q \cdot (r_m + x)] \cdot \rho(x)\mathrm{d}x \int_{(d_L/2)}^{d_L/2} \cos[q \cdot (r_m + x)] \cdot \rho(x)\mathrm{d}x = \cos(q r_m) \cdot \rho(q) \tag{10}$$

with

$$\rho(q) = \rho^{\mathrm{strip}}(q) = \frac{2}{q} \cdot \left[(\rho_h - \rho_s) \cdot \sin\left(q \cdot \frac{d_L}{2}\right) + (\rho_c - \rho_h) \cdot \sin\left(q \cdot \frac{c}{2}\right)\right] \tag{11a}$$

and

$$\rho(q) = \rho^{\mathrm{boat}}(q) = \frac{2}{q} \cdot (\rho_c - \rho_s) \cdot \left\{ \sin\left(q \cdot \frac{d_L}{2}\right) \cdot \frac{\sin(q \cdot h)}{q \cdot h} + \cos\left(q \cdot \frac{d_L}{2}\right) \cdot \frac{\left(1 - \cos\left(q \cdot \frac{d_L}{2}\right)\right)}{q \cdot h} \right\} \tag{11b}$$

in case of the strip and the boat model, respectively.

The summation in (7) can be performed using the formula

$$\sum_{m=0}^{M-1} \cos(q r_m) = \cos\left[q \cdot \left(r_0 + (M-1) \cdot \frac{d}{2}\right)\right] \cdot \frac{\sin\left(\frac{qMd}{2}\right)}{\sin\frac{qd}{2}} \tag{12}$$

giving

$$F_m(q) = \left(\frac{4\pi}{q}\right) \cdot \left(\frac{-\partial}{\partial q}\right)\{\cos(r_{0M}) \cdot f_M(q)\}$$

Here $r_{0M} = r_0 + (M-1) \cdot \frac{d}{2}$ is the radius of the vesicle consisting of M bilayers with r_0 as the midpoint radius of the innermost bilayer in the vesicle, and

$$f_M(q) = \rho(q) \cdot \frac{\sin\left(\frac{qMd}{2}\right)}{\sin\left(\frac{qd}{2}\right)}.$$

The average coherent cross section of the M-vesicles is given by the averaged squared absolute value of the scattering amplitude:

$$I_M^{\mathrm{coh}}(q) = \left\langle |F_M(q)|^2 \right\rangle = \left(\frac{4\pi}{q}\right) \cdot \left\langle \left[r_{0M} \cdot \sin(q r_{0M}) \cdot f_M(q) + \cos(q r_{0M}) \cdot \left(\frac{-\partial}{\partial q}\right) f_M(q) \right]^2 \right\rangle \tag{14}$$

The second term in the brackets can be neglected with respect to the first one in case of $r_{0M} \gg d$, giving (1).

Appendix 2: Averaging over vesicle-radius distribution

Using the integral (Gradshtein and Ryzhik 1971)

$$\int_0^\infty x^{\mu-1} e^{-\beta \cdot x} \cos(\delta \cdot x) \mathrm{d}x = \frac{\Gamma(\mu)}{\left(\delta^2 + \beta^2\right)^{\frac{\mu}{2}}} \cdot \cos\left(\mu \cdot \arctan\left(\frac{\delta}{\beta}\right)\right)$$

the averaging over the radius distribution in (1) can be performed readily giving

$$\left\langle r_{0M}^2 \cdot \sin^2(q \cdot r_{0M}) \right\rangle = \frac{5}{8} R^2 \cdot \left\{1 + \xi^3 \cdot \left[1 - 18 \cdot \xi + 48 \cdot \xi^2 - 32 \cdot \xi^3\right]\right\}$$

with

$$\xi = \frac{1}{1 + \left(\frac{q \cdot R}{2}\right)^2}$$

References

Cornell BR, Fletcher GC, Middlehurst J, Separovic F (1981) Temperature dependence of the size of phospholipids vesicles. Biochim Biophys Acta 642:375–380

Engelhaaf SU, Wehrli E, Müller M, Adrian M, Schurtenberger P (1996) Determination of the size distribution of lecithin liposomes: a comparative study using freeze fracture, cryoelectron microscopy and dynamic light scattering. J Microsc 184:214–228

Fromherz P (1983) Lipid-vesicle structure: size control by edge-active agents. Chem Phys Lett 94:259–265

Gabriel NE, Roberts MF (1984) Spontaneous formation of stable unilamellar vesicles. Biochem 23:4011–4015

Gradshtein IS, Ryzhik IM (1971) Tables of integrals (in Russian). Nauka, Moscow

Hallett FR, Nickel B, Samuels C, Krygsman PH (1991) Determination of vesicle size distributions by freeze-fracture electron microscopy. J Electr Microsc Tech 17:459

Hope MJ, Bally MB, Webb G, Cullis PR (1985) Production of large unilamellar vesicles by a rapid extrusion procedure. Characterization of size distribution, trapped volume and ability to maintain a membrane potential. Biochim Biophys Acta 812:55–65

Kiselev MA, Lesieur P, Kisselev AM, Lombardo D, Killiany M, Lesieur S (2001) Sucrose solutions as prospective medium to study the vesicle. J Alloys Compd 328:71–76

Mayer LD, Hope MJ, Cullis PR (1986) Vesicles of variable sizes produced by a rapid extrusion procedure structure: SAXS and SANS study. Biochim Biophys Acta 858:161–168

Nelder JA, Mead R (1965) A simplex method for function minimization. Comput J 7:308

New RRC (1990) Liposomes: a practical approach. IRL Press, Oxford

Pedersen J S, Posselt D, Mortensen K (1990) Analytical treatment of the resolution function for small-angle scattering. J Appl Cryst 23:321–333

Rosta L (2002) Cold neutron research facility at the Budapest Neutron Centre. Appl Phys A74[Supp l.]:S52–S54

Schmiedel H, Jörchel P, Kiselev M, Klose G (2001) determination of structural parameters and hydration of unilamellar POPC/$C_{12}E_4$ vesicles at high water excess from neutron scattering curves using a novel method of evaluation. J Phys Chem B 105:111–117